

Microsaccades are modulated by both attentional demands of a visual discrimination task and background noise

Laboratoire de Psychologie et NeuroCognition,
University Grenoble Alpes, Grenoble, France
Department of Medicine, University of Fribourg,
Fribourg, Switzerland

Halim Hicheur



Steeve Zozor

Grenoble-Image-Parole-Signal-Automatique (GIPSA-lab),
University Grenoble Alpes, Grenoble, France



Aurélie Campagne

Laboratoire de Psychologie et NeuroCognition,
University Grenoble Alpes, Grenoble, France



Alan Chauvin

Laboratoire de Psychologie et NeuroCognition,
University Grenoble Alpes, Grenoble, France



Microsaccades are miniature saccades occurring once or twice per second during visual fixation. While microsaccades and saccades share similarities at the oculomotor level, the functional roles of microsaccades are still debated. In this study, we examined the hypothesis that the microsaccadic activity is affected by the type of noisy background during the execution of a particular discrimination task. Human subjects had to judge the orientation of a tilted stimulus embedded in *static* or *dynamic* backgrounds in a forced choice-task paradigm, as adapted from Rucci, Iovin, Poletti, and Santini (2007). Static backgrounds induced more microsaccades than dynamic ones only during the execution of the discrimination task. A directional bias of microsaccades, dictated by the stimulus orientation, was temporally coupled with this period of increased activity. Both microsaccade rates and orientations were comparable across background types after the response time although subjects maintained fixation until the end of the trial. This represents a background-specific modulation of the microsaccadic activity driven by attentional demands. The visual influence of microsaccades on discrimination performances was modeled at the retinal level for both types of backgrounds. A higher simulated microsaccadic activity was necessary for static backgrounds in order to achieve discrimination performance scores comparable to that of dynamic ones. Taken together, our experimental and theoretical findings further support the idea that microsaccades are under attentional control and

represent an efficient sampling strategy allowing spatial information acquisition.

Introduction

Visual fixation is accompanied by miniature eye movements called fixational eye movements (FEMs). Three types of FEMs (drift, tremor, and microsaccades) can be distinguished (Rolfs, 2009). Microsaccades are particularly remarkable among FEMs as they share several kinematic properties with larger saccades. Besides, converging evidence suggests that microsaccades and saccades are generated by the same neuronal structures (Hafed, Goffart, & Krauzlis, 2009; Van Horn & Cullen, 2012). Models accounting for the generation and modulation of the microsaccadic activity at the level of subcortical areas (e.g., superior colliculus, premotor nuclei, and motor neurons) were described over the past years (Engbert, Mergenthaler, Sinn, & Pikovsky, 2011; Hafed, 2011; Otero-Millan, Macknik, Serra, Leigh, & Martinez-Conde, 2011).

Yet, the functional role of microsaccades was questioned in early studies: Steinman, Haddad, Skavenski, and Wyman (1973) observed that the control of fixation position was not altered in absence of microsaccades. Winterson and Collewijn (1976) recorded microsaccades during a "threading a needle" task and

observed that microsaccade rates decreased just before the end of the trial, suggesting that microsaccades were detrimental to performance.

In contrast, several groups provided evidence that microsaccades are anything but oculomotor noise. For instance, Ko, Poletti, and Rucci (2010) replicated the “threading a needle” task in a highly controlled virtual environment and observed that the frequency of occurrence of the smallest microsaccades significantly increased near the completion of the task, while they were rare during threading or fixation. Microsaccades clearly relocated the line of sight back and forth between the thread and the needle. Microsaccades also reflect shifts of spatial attention as evidenced by the correlation between microsaccade directions and attended stimuli (Engbert & Kliegl, 2003; Engbert, 2012; Hafed & Clark, 2002; Hafed, Lovejoy, & Krauzlis, 2011; Pastukhov, Vonau, Stonkute, & Braun, 2013). Microsaccades are also useful for the prevention of fading (Martinez-Conde, Macknik, Troncoso, & Dyar, 2006; see also McCamy et al., 2012; but see Poletti & Rucci, 2010). Using a method of retinal image stabilization, Rucci, Iovin, Poletti, and Santini (2007) showed that observers better discriminate the tilt of high spatial frequency gratings (embedded in low-pass filtered noise) in the unstabilized condition compared to the stabilized one. In the latter condition, any retinal image motion generated by FEMs was compensated in the visual display, leading to retinal image stabilization. While these authors clearly described how FEMs facilitate gratings discrimination, the different types of FEMs were not distinguished in this study. This was recently done by Poletti, Listorti, and Rucci (2013) who showed that discrimination of fine patterns is indeed improved by microsaccades.

Here, we examined how the microsaccadic activity might be modulated by attentional demands in order to enhance discrimination performance. To this purpose, we adapted the paradigm designed by Rucci et al. (2007) where human observers had to judge the orientation of *high* or *low* spatial frequency stimuli (versus *static* or *dynamic* backgrounds in our study) during fixation. As mentioned above, the microsaccades-induced retinal motion might facilitate discrimination of stimuli embedded in static backgrounds (Rucci et al., 2007). Accordingly, we would expect less microsaccades when such task is performed in presence of *dynamic* backgrounds.

Theoretically, any dynamic change occurring in a tiny visual region may be helpful for stimulus discrimination. This was recently modeled using a basic model of retinal photoreceptors (Zozor, Amblard, & Duchene, 2009). In the last part of our study, we implemented a modified version of this model where we simulated the microsaccades effects on discrimination performances.

Methods

Thirty participants (20 females and 10 males, with normal or corrected-to-normal vision, ranged from 18 to 45 years of age) provided written consent prior to their inclusion in the study. Except for the four coauthors, all other participants were naïve as to the purpose of the study. Our experiments conformed to the Code of Ethics of the 1964 Declaration of Helsinki. Each subject performed a total of four experiments: the first two experimental blocks consisted in pre-experiments where we assessed individual discrimination thresholds that were used in the following blocks where eye movements were recorded. All experiments took place on the same day and were separated by at least 5 min rest periods. A first training session of 10 to 30 trials was run in order to familiarize subjects with the task.

Setup

Experiments took place in a dark room. Participants were seated in front of a 22 in., Iiyama (Vision Master Pro 513-MA203DT, resolution: 1024×768 pixels, refresh rate: 100 Hz, and brightness: 63 cd/m^2) CRT monitor at a distance of 66 cm. They had to place their head on a chinrest whose position was adjusted so that the midpoint between the two eyes was centered on the screen. Eye movements were recorded binocularly with an Eyelink 1000 Desktop system (SR Research Ltd., Kanata, Ontario, Canada) running at a sampling rate of 1000 Hz, with a resolution equal to 0.01° (manufacturer estimation). A standard nine-point calibration was performed systematically before every experiment and after 40 trials within a single experimental block. Drift correction was performed every three trials.

Experimental paradigm

We adapted the discrimination task designed by Rucci et al. (2007). In their study, subjects had to judge between two possible orientations of a grating perturbed by noise (at high or low spatial frequency). Here, we used ellipses (rather than gratings, see below for more details about the visual stimulus) with high-spatial-frequency textures. Besides, we tested two stimulus sizes and displayed the stimulus for longer durations (5 s instead of 1 s in Rucci study). This was done both to maintain sustained attention towards the visual stimulus and to get a sufficient number of microsaccades for the subsequent analyses. The timing of this forced-choice task was organized as depicted in Figure 1A.

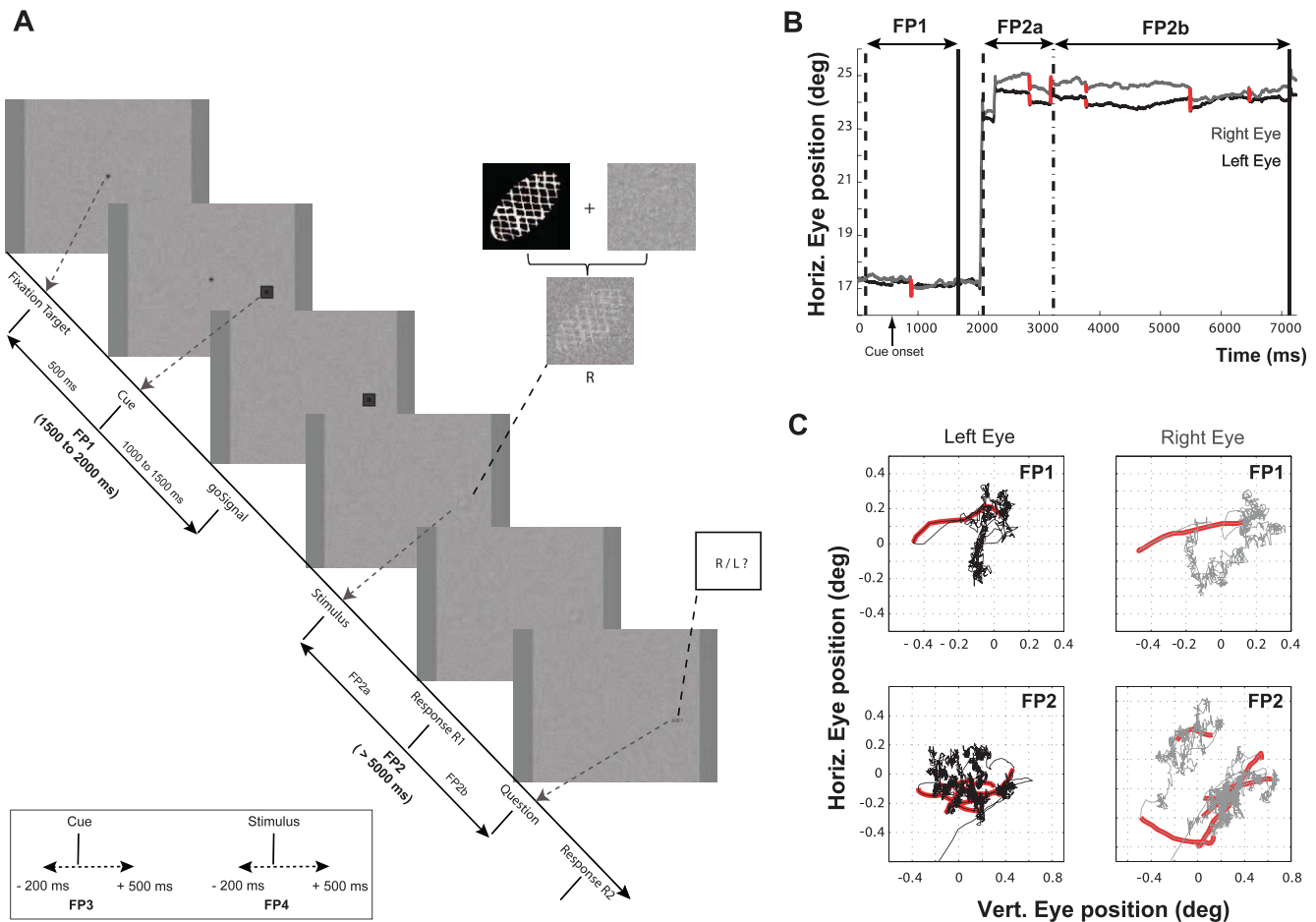


Figure 1. (A) Forced-choice task illustrated for a single trial: Subjects made a saccade to the cued target (black square) when the initial fixation target (small black dot) disappeared. Subjects first judged the stimulus orientation (R or L, see text for details) at R1. The stimulus consisted of a textured ellipse embedded into a static or dynamic noisy background. Subjects then maintained fixation until the appearance of the question window, after which subjects had to confirm/change their first response (R2). Bottom-left corner: Fixation periods FP3/FP4 defined relatively to cue/stimulus presentation. (B) Binocular eye positions recorded during the time course of a single trial: red traces correspond to the detected microsaccades; dashed and continuous vertical lines correspond to the beginning and end of FP1 and FP2. The dashed-dot central line corresponds to the response R1 which delimits FP2a and FP2b subperiods. (C) Fixational eye movements during the initial period FP1 (top) or during the stimulus fixation period FP2 (bottom); red traces correspond to binocular microsaccades detected for the trial illustrated in (B).

For each trial, the cue eccentricity and direction (Figure 1A) were extracted from a uniform random distribution with values ranging from 5.9° to 11° , and from 0° to 360° , respectively. As soon as the fixation target disappeared, subjects executed a saccade to the cue location, as in Rucci's original paradigm (Rucci et al., 2007). The stimulus appeared only if the eyes were located inside the stimulus window (for at least 20 ms). Subjects had then to press a button on the keyboard in order to report whether the stimulus was tilted clockwise or counterclockwise (using the right and left buttons, respectively). Importantly, subjects had to maintain fixation on the stimulus until the appearance of a question Q (see Figure 1A). We integrated the question Q in order to increase the duration of the stimulus fixation (without Q, subjects tended to

systematically generate a saccade out of the stimulus window few hundreds of milliseconds after R1, as tested in preliminary experiments). A single experimental block was composed of 80 trials and lasted between 12 and 16 min, including the rest, re-calibration and drift correction periods.

Visual stimulus

The *noise-free* stimulus consisted of a textured ellipse I_{nf} with high-spatial-frequency texture (Brodatz, 1966, see Figure 1A). Importantly, the high-spatial frequency texture by itself did not allow inferring the ellipse orientation. In each trial, the ellipse had equal probability ($\Pr[I_{nf} = I_{cw}] = \Pr[I_{nf} = I_{ccw}] = \frac{1}{2}$) of being

tilted by -45° ($I_{nf} = I_{cw}$ where cw stands for clockwise) or $+45^\circ$ ($I_{nf} = I_{ccw}$ where ccw stands for counterclockwise). It was embedded in a squared window (size = 2° and 3.3° of visual angle, for the SMALL and BIG stimuli, respectively). The 30 tested subjects were divided into two groups (18 and 17 subjects for the SMALL and BIG stimuli—five subjects performed both experiments). The stimulus size was used as a control parameter. The minor and major axes of the ellipse represented a quarter of and half of the side length of the squared window, respectively. The background inside the squared window was computed using a uniform white noise $U(x, t)$. We then computed the (noisy) visual stimulus $I(x, t)$ as follows:

$$I(x, t) = c \cdot I_{nf}(x) + (1 - c) \cdot U(x, t) \quad (1)$$

where c is the noise-free stimulus contrast coefficient. Importantly, the contrasts of both the noisy stimulus and the visual background were kept constant across sessions and subjects.

Experimental conditions

Both groups were tested in two conditions (static and dynamic, Figure 1A). In the dynamic one, a new noise field $U(x, t)$ was generated every frame (every 10 ms, in an independent manner) while a single noise field $U(x, t) = U(x, t_0)$ was used in the static condition. The coefficient c was assessed individually for every subject and conditions during the pre-experiments: it was changed on a trial-by-trial basis following a QUEST procedure (Watson & Pelli, 1983) so that percentages of correct stimulus discrimination settled around 82%. A single coefficient c_s or c_d was used for each subject during the experiments for the static and dynamic conditions, respectively. In order to avoid any potential bias, the order of both pre-experiments and experiments were counterbalanced across subjects.

Eye movement analyses

Definition of the fixation periods

For each trial, we extracted microsaccades for two particular fixation periods (FP1 to FP4, see Figure 1). FP1 was defined as the initial target fixation and lasted as long as the target fixation was displayed on the screen (from 1500 to 2000 ms). We used FP1 as a baseline because this period was identical (in terms of visual stimulation) across conditions. FP2 was the fixation period during stimulus exposure (i.e., from stimulus appearance to Q) and lasted 5 s at least. We defined FP3 and FP4 around cue appearance or around stimulus presentation, respectively (see bottom-left corner in Figure 1A): both had a fixed duration of 700

ms. It should be noticed that FP4 included the (large) saccade to the cued location: This saccade was excluded from the analysis (except for the computation of the main sequence). Since blinks were unavoidable for the long fixation periods, rejecting trials with blinks would have led us to exclude a significant part of the experimental data. Rather, we excluded data recorded 50 ms before and after blink occurrences (detected as the instants where pupil information was missing) from the analyzed fixation periods (see also McCamy et al., 2012).

Detection of saccades and microsaccades

The fixation-to-stimulus saccade events were detected using either the Eyelink software saccades-detection algorithm or using a self-written MATLAB routine based on the root mean square deviation of the 2-D distance D_{e-s} between the eye position and the stimulus location. D_{e-s} was computed over a time interval starting at $t_0 = \text{goSignal}$ (beginning of FP1, see Figure 1B) and ending at $t_1 = \text{R1}$ (end of FP2a). Within this interval, we looked for systematic deviations in D_{e-s} over 200 ms bins: The fixation-to-stimulus saccadic period was first detected as the bin for which the standard deviation of D_{e-s} exceeded 1° (a nonfixation period). This particular bin was then split in 20 ms bins and 20 ms nonfixation periods were then detected using the same algorithm. The beginning and end of the fixation-to-stimulus saccade were extracted from these 20 ms nonfixation periods. This procedure provided slightly better temporal accuracy compared to the Eyelink algorithm, as observed after a visual inspection of all fixation-to-stimulus saccadic periods.

Microsaccades were detected for all fixation periods using the algorithm developed by Engbert and Merzenicher (2006). Only binocular saccades/microsaccades were considered (see Figure 1C). They were defined as epochs lasting at least 10 ms in which the relative threshold multiplier was fixed to four. In addition, we imposed a minimum intersaccadic interval of 25 ms so that potential overshoot corrections were not detected as new saccades. Similarly, any microsaccade detected in the 50 ms following the end of the fixation-to-stimulus saccade was considered as a corrective saccade and was excluded from the analysis. Any saccade with amplitude smaller than 1° was categorized as a *microsaccade* (saccades with amplitudes smaller than 2° were considered in a second stage of our analysis, see Results section). We visually inspected all saccades/microsaccades detected according to this procedure. We then plotted the main sequence of saccades and microsaccades (Figure 2A1 and B1) and observed, in agreement with previous studies (e.g., Zuber, Stark, & Cook, 1965), that both share the same magnitude/peak velocity relationship.

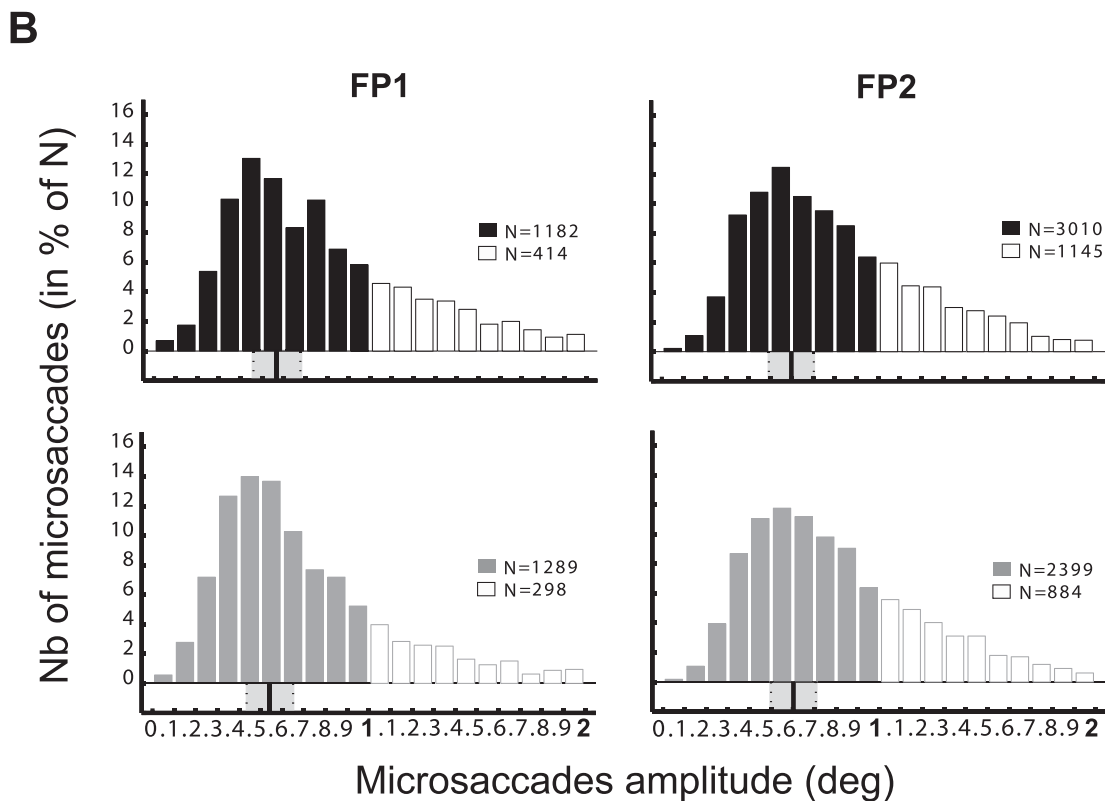
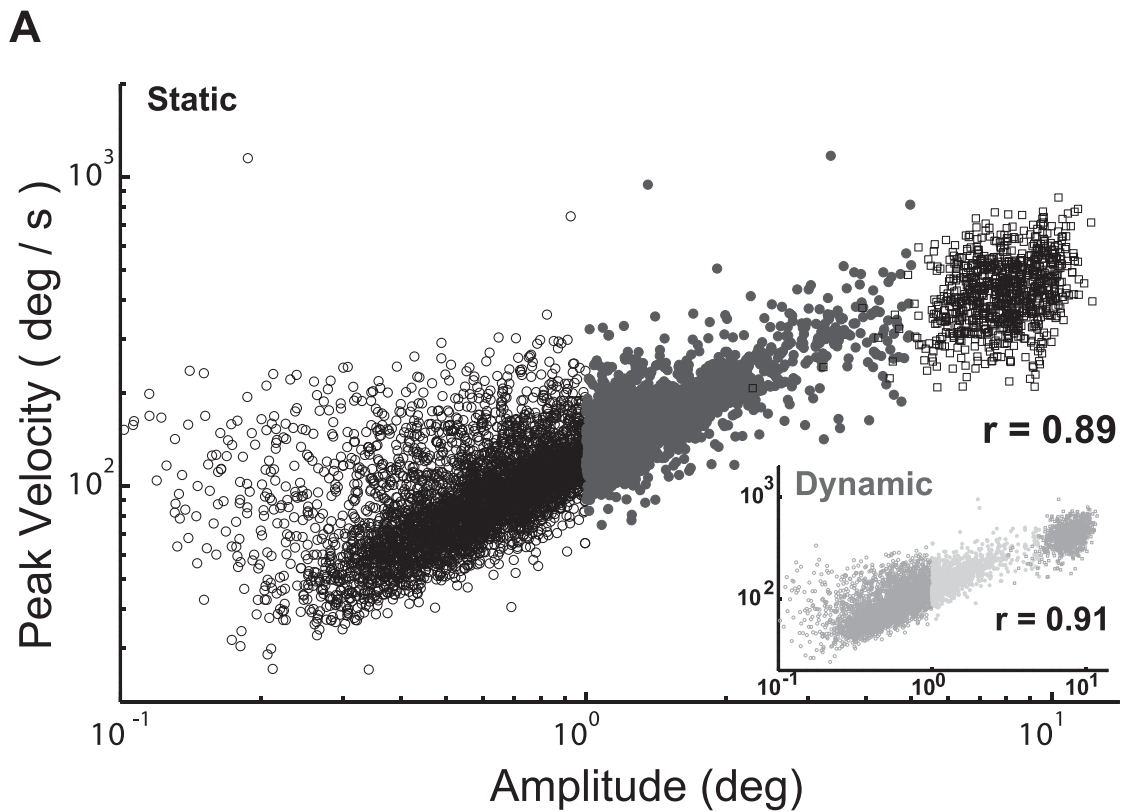


Figure 2. (A) Main sequence: relationships between saccades amplitudes and peak velocities (all microsaccades and saccades pooled together) in the static and dynamic conditions. (B) Distribution of saccade amplitudes during fixation periods FP1 and FP2. The mean (vertical thick line) and \pm SD (gray square around the mean) are provided under the histograms. Bars with (black/gray)/white font correspond to microsaccades with amplitude smaller/larger than 1° , respectively. These two groups of (micro)saccades were separately analyzed (see text for details).

Microsaccades properties (rate, amplitude, and direction)

We computed the rate, amplitude, and directions of microsaccades for each of the fixation periods FP1 and FP2. FP2 was also divided in fixation subperiods FP2a and FP2b: FP2a was defined as the interval between the stimulus presentation and R1 while FP2b was defined as the interval between R1 and Q (see Figure 1A, B).

Microsaccade rate signature

Engbert and Kliegl (2003) reported a systematic drop in the microsaccade rate around 150 ms after cue onset and a peak around 350 ms after cue onset. We computed this microsaccade rate signature for all periods of interest: the frequency of occurrence of microsaccades was averaged over all trials of the subjects within windows of 80 ms moved in 1 ms steps. The variability around the mean curves was estimated using the 95% confidence intervals by computing bootstraps of the entire array of the microsaccades distribution (500 iterations with replacement, see Hafed, Lovejoy, & Krauzlis, 2013).

Directional bias of microsaccades

We computed the relative angle between the microsaccade vector and the line defined by the fixation target and the cue location (periods FP1/FP3). We also computed the angle between the microsaccade vector and the major axis of the ellipse (defining the stimulus orientation) in order to examine the potential effect of the stimulus on the microsaccade directions (FP2/FP4). We further analyzed the distribution of microsaccade directions using the circular statistics toolbox for Matlab (Berens, 2009) and searched for a potential directional bias towards the direction of the cue target (Engbert & Kliegl, 2003; Hafed & Clark, 2002) or in the direction of the ellipse orientation. We observed two main types of microsaccade direction distributions: *axial* and *non-axial* distributions. Axial distributions were identified as distributions with two or four modes (with biases towards specific directions, e.g., one of the directions mentioned above or oblique directions). We performed a Hodges-Ajne test to statistically confirm that these distributions were not uniform. In few cases with small sample size (2 out of 40), the hypothesis of uniformity could not be rejected. In the case of bimodal/quadrmodal distributions, we multiplied the angular values by two/four before computing the mean resultant vector of the distributions (Berens, 2009; Jammalamadaka Rao & SenGupta, 2001). Non-axial distributions were characterized by a rough bias towards a particular direction associated with weaker biases in the opposite oblique directions. This was observed for 6 out of 40 distributions where the Hodges-Ajne test did not detect any significant

deviation from uniformity. We computed here the median of the distribution and compared it to this particular direction to test if the bias was significant. We then computed the mean (as well as the 95% confidence intervals, or the median) angular directions between static and dynamic conditions (Berens, 2009; Jammalamadaka Rao & SenGupta, 2001). This was done using a (parametric) Watson-Williams multi-sample test for equal means (the circular analogue of a one-factor analysis of variance [ANOVA]) or using a (non-parametric) multisample test for equal median directions (the circular analogue of a Kruskal-Wallis test).

Statistical analysis

We performed mixed analysis of variance (ANOVA) using Statistica 5.1 software package (Statsoft®) on the discrimination performances, the noise-free stimulus contrast coefficients, mean microsaccade rates, and amplitudes, with two groups (SMALL and BIG) and four within factors (two conditions—static and dynamic— \times 2 fixation periods—FP1 and FP2). Comparisons were also separately performed for five subjects who participated in both experimental sessions: SMALL and BIG here were computed as within factors. We compared the amplitudes/rates ratios (static/dynamic) between different fixation periods using Newman-Keul tests for post-hoc comparisons. Because most of the comparisons between the SMALL and BIG stimuli were not found to significantly differ (see also Thaler, Schütz, Goodale, & Gegenfurtner, 2013), only results obtained for the BIG stimulus are presented. Nevertheless, we systematically included the SMALL data (see above) in the statistical comparisons: Any difference between the SMALL and BIG stimuli is mentioned in the text.

Results

The changes in microsaccadic activity and their relation to the discrimination task were examined here. Our task had two components: an initial fixation period (FP1) with a peripheral cue that instructed a later saccade and a subsequent one (FP2) during which subjects had to judge a visual stimulus. The initial period was comparable to the one used in classic cueing experiments (see Introduction), where microsaccades properties are affected by the cue onset. This is what we found in our own data, as summarized in the first part of this section. In contrast, we will detail here new findings observed during task execution (FP2) where consistent stimulus-driven microsaccadic changes were

observed. A computational approach accounting for these findings is proposed in the last part of this section.

Discrimination performances

The mean discrimination performances were equal to $84.4\% \pm 11.3\%$ and $87.9\% \pm 13.2\%$ of correct responses in the static and dynamic conditions (respectively) and were not found to significantly differ ($p > 0.05$). This performance level was slightly higher than that fixed in the pre-experiments (82%). This might be explained by the fact that subjects first performed the pre-experiments and became more familiar with the discrimination task when performing the experiments. Besides, subjects confirmed their first judgment (R1) at the end of stimulus presentation: the response R1 was similar to the response R2 in in $96.2\% \pm 3.0\%$ and $96.9\% \pm 4.0\%$ of the trials in the static and dynamic conditions, respectively. The noise-free contrast coefficient evaluated in the pre-experiments was smaller, $F(1, 33) = 181$, $p < 0.001$, in the dynamic condition, ($c_d = 0.05 \pm 0.01$) than in the static one ($c_s = 0.11 \pm 0.02$). Thus, a higher contrast coefficient in the static condition was necessary in order to obtain performances comparable to that of the dynamic one. Almost all subjects orally reported that the task was more demanding in the static condition.

Microsaccade properties

Microsaccade amplitudes and peak velocities

As depicted in Figure 2A, saccades and microsaccades distributions follow the same main sequence (Zuber, Stark, & Cook, 1965). The shape of these distributions was not affected by the background noise (static or dynamic). The correlation coefficient between the amplitude and the peak velocity of (micro)saccades was around 0.9 across stimulus sizes and backgrounds. The distribution of microsaccade amplitudes was positively skewed both for the initial fixation period FP1 (Figure 2B, left panel, mean = 0.56) and for the stimulus fixation period FP2 (Figure 2B, right panel, mean = 0.66). Saccades with amplitude larger than 1° belong to the same distribution, irrespective of the background type. Here, we observed an effect of the stimulus size on the microsaccade amplitude (mean = 0.67° and 0.72° for FP1 and FP2 in the case of the SMALL stimulus). This effect was significant for both FP1, $F(1, 33) = 19.8$, $p < 0.01$ and FP2, $F(1, 33) = 12.1$, $p = 0.04$, periods. This was surprising because the size of the initial fixation control window was identical in SMALL and BIG groups. In fact, the difference was not statistically significant for both fixation periods ($p > 0.05$) when performing the comparison only for the

five subjects who participated in both experiments. Finally, background noise did not affect the microsaccade amplitude ($p > 0.05$), whatever the fixation period. In the next sections, we examine the properties of microsaccades defined using the 1° amplitude criterion (the black and gray bars in Figure 2B).

Microsaccade rate evolution around a sudden visual event

The presentation of a sudden visual transient during fixation induces a drop in the microsaccade rate about 150 ms after cue onset followed by a rebound phase 150 ms later (Engbert & Kliegl, 2003). We observed this typical signature around both peripheral cue (period FP3, not shown) and stimulus (period FP4) presentations. A stronger rebound phase was observed in the static condition compared to the dynamic condition around 250 ms post-stimulus presentation (see Figure 3A). It should also be noted that the baseline level of microsaccade rates observed in our study (around 0.5 microsaccades/s) is comparable to the one reported in some studies (Ko et al., 2010; McCamy et al., 2012) but smaller than the one observed in other studies (Engbert & Kliegl, 2003; Engbert et al., 2011): the different paradigms tested (e.g., type of task, fixation duration, etc.) can account for these quantitative differences.

Microsaccadic activity during the execution of the discrimination task

Here, we examined how long-lasting attentional demands of a particular discrimination task affect the microsaccadic activity. Below is a description of the main spatial and temporal attention-related changes in the microsaccadic activity as a function of the type of background noise and discrimination performance.

Attention-related temporal changes

We observed that the short-term modulation of the microsaccade rate (the rebound phase previously described) was followed by a sustained higher microsaccade rate in the static condition for nearly 2 s after stimulus presentation (Figure 3A). The mean rate in the static condition then progressively decreased to reach the level of the dynamic condition. We plotted the distribution of the reaction times in the two conditions (Figure 3A) in order to illustrate the fact that this initial period of microsaccadic enhancement coincided with the execution of the discrimination task for most of the subjects.

This was further quantified in the histograms shown in Figure 3B (left panel) where the ratios between the mean microsaccade rates of the two conditions were

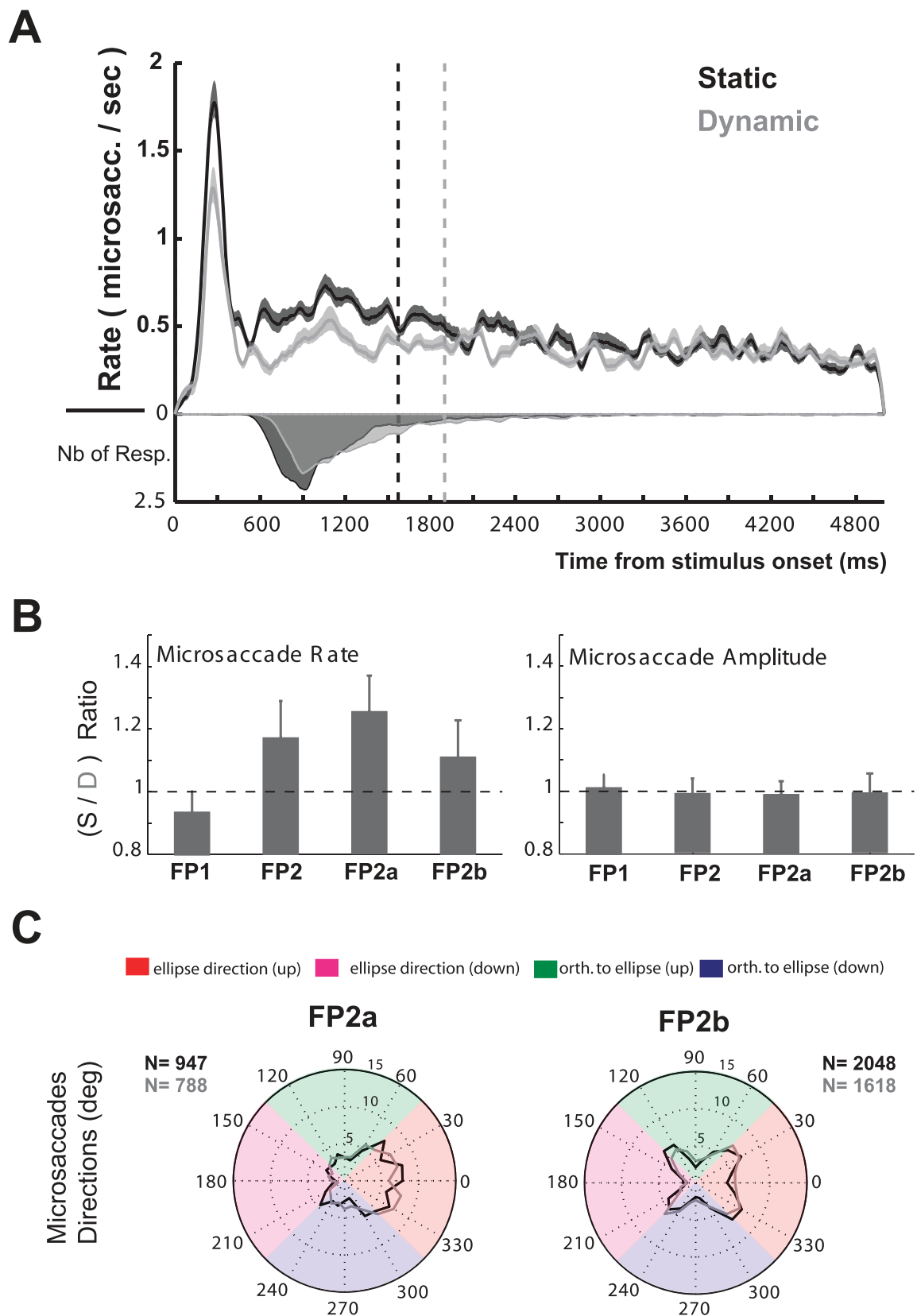


Figure 3. (A) Evolution of the microsaccade rate for the whole stimulus fixation period FP2 for static and dynamic conditions. The response times distributions are depicted under the horizontal axis. The stimulus was presented at $t = 0$; dashed vertical lines correspond to instants where at least 85% of the responses were provided: Note that the microsaccade rate is higher in the static

→

←
condition and progressively converges towards that of the dynamic one. (B) Static/dynamic ratios for microsaccade rates (left panel) and amplitudes (right panel) for different fixation periods. FP1 is a control period (no stimulus). FP2a and FP2b are subperiods of FP2, delimited by first subject responses R1 (see Figure 1A and B). Note the higher microsaccade rate for the static condition during FP2: this was mainly due to the period FP2a. (C) Distribution of microsaccade orientations for FP2a (left panel) and FP2b (right panel): Note the bias in FP2a distributions where microsaccades were directed more in the ellipse orientation compared to FP2b where they were equally distributed along oblique directions during FP2. See also Table 1 for results of the circular statistics analysis.

computed for the periods FP1 (control—no stimulus), FP2, FP2a, and FP2b. The static/dynamic microsaccade rate ratio was close to one for FP1 (Figure 3B, left panel): this is not surprising since FP1 was used as a baseline where no noisy background was present (see Methods). In contrast, the microsaccade rate was 20% higher for FP2 compared to FP1, $F(1, 33) = 11.56, p = 0.0018$. This microsaccadic enhancement was stronger during FP2a (up to 35% higher than in FP1) and weaker during FP2b (around or less than 15% higher than in FP1). The Newman-Keuls post-hoc comparisons revealed significantly higher rates during FP2a compared to FP1 ($p < 0.01$ for both stimulus sizes). It is striking to observe such a difference in the microsaccade rate between FP2a and FP2b. Indeed, subjects were exposed to the same visual stimulus for the whole FP2 period. Since FP2a precisely ended at the time where subjects delivered their first response R1, this first microsaccadic enhancement was clearly linked to the execution of the discrimination task. We further addressed this issue by quantifying a potential change in the microsaccades amplitudes and/or directions across these periods. The rationale for this is that if microsaccades helped in better discriminating the ellipse orientation, this may also be reflected in the spatial attributes of microsaccades.

Attention-related spatial changes

The mean static/dynamic amplitude ratios observed across subjects and periods are presented in the Figure 3B (right panel). They were close to one and did not significantly differ across periods ($p > 0.05$). Besides, the mean microsaccade amplitude was not found to be affected by the type of noise present in the background ($p > 0.05$, see also the distributions of microsaccade amplitudes in Figure 2B). In contrast, we observed significant changes at the level of microsaccade orientations during the time course of task execution. Indeed, microsaccades in the direction of the major axis of the ellipse were more frequent than microsaccades in other directions for the whole FP2a period only (Figure 3C, left panel, see all the results of the circular statistics analyses for the “all” group in Table 1). In contrast, we observed multimodal distributions with clear biases towards oblique directions during FP2b (after R1:

Figure 3C, right panel). Oblique directions (relatively to the stimulus orientation) corresponded to absolute horizontal and vertical directions on the screen, a type of bias already reported in the literature (see Engbert, 2006, for a review). Interestingly, background noise was not found to significantly affect microsaccade direction distributions across fixation periods (with one exception, see Table 1 all group).

Differential effect of the discrimination task on saccades with different amplitudes

The observations presented so far were obtained for saccades with amplitude smaller than one degree, a threshold used in many recent studies (see Colleijn & Kowler, 2008). Here, we sorted (micro)saccades in three categories, depending on their amplitudes: very small (VS), medium (MS), and larger (LS) saccades had amplitudes ranged between 0.1° and 0.5° , 0.5° and 1° , and between 1° and 2° , respectively. This was done by setting the amplitude threshold (see Methods) to different values. The VS inferior limit was fixed to 0.1 , following Colleijn and Kowler (2008) who questioned the accuracy of eye trackers in detecting microsaccades smaller than 5 min of arc (around 0.083°).

Attention-related temporal changes

The static/dynamic saccade rate ratio was found to be systematically affected during the discrimination task only (FP2a period) in the static condition. The microsaccade rate was more than 30% higher for VS and MS saccades (Figure 4A1, B1, top panel) and more than 10% higher for LS saccades (Figure 4C1, top panel). These differences were statistically significant for all categories except LS, $F(1, 25) = 7.99, p < 0.001$, $F(1, 32) = 13.56, p < 0.001$, and $F(1, 29) = 0.15, p > 0.05$ for the VS, MS, and LS saccades, respectively. Note here that the difference was not significant for VS saccades of the SMALL group ($p > 0.05$). Similarly, the microsaccade rate ratio was significantly higher during FP2a compared to FP2b only for VS and MS saccades, $F(1, 25) = 12.27, p < 0.01$ and $F(1, 32) = 4.73, p = 0.037$, respectively.

Directional bias (degrees)	FP2a			FP2b			FP2a			FP2b			FP2a			FP2b			
	To. Ellipse			Multi. bias			To. Ellipse			Multi. bias			No bias			Multi. bias			
	St.	Dy.		St.	Dy.		St.	Dy.		St.	Dy.		St.	Dy.		St.	Dy.		
SMALL																			
N	736	702	1403	1102	112	99	257	155	612	599	1137	935	438	590	541	349			
Mean/ Median	-16.3	4.79	—	—	-13.17	-10.84	—	—	-16.9	5.54	—	—	—	—	—	—			
C.I./p	$p < 0.01$	$p = 0.38$	—	—	$p = 0.56$	$p = 0.84$	—	—	$p < 0.01$	$P = 0.28$	—	—	—	—	—	—			
Noise	$P(1437) = 5.39$	$F(1, 2503) = 0.65$	$p = 0.42$	—	$P(210) = 0.12$	—	$F(1, 410) = 1.31$	—	$P(1210) = 5.97$	—	$F(1, 2070) = 0.04$	—	$F(1, 1026) = 1.72$	—	$F(1, 888) = 0.68$	—			
Comparison	$p = 0.02$	—	—	—	$p = 0.73$	—	$P = 0.25$	—	$p = 0.014$	—	$p = 0.83$	—	$p = 0.19$	—	$p = 0.41$	—			
	— *	—	—	—	—	—	—	—	— *	—	—	—	—	—	—	—			
BIG																			
N	947	788	2048	1618	210	222	794	579	726	568	1227	1021	426	422	672	429			
Mean/ Median	-1.19	0.56	—	—	4.17	-10.4	21.8	4.8	-3.34	2.73	—	—	—	—	—	—			
C.I./p	$[-10, 8]$	$[-9, 8]$	—	—	$[-15, 24]$	$[-29, 8]$	$p < 0.01$	$P = 0.56$	$[-14, 7]$	$[-7, 13]$	—	—	—	—	—	—			
Noise	$F(1, 1733) = 0.63$	$F(1, 3664) = 1.35$	$p = 0.25$	—	$F(1, 430) = 0.1$	—	$P(1372) = 2.58$	—	$F(1, 1292) = 1.43$	—	$F(1, 2246) = 0.09$	—	$F(1, 846) = 3.64$	—	$F(1, 1099) = 0.06$	—			
Comparison	$p = 0.43$	—	—	—	$p = 0.75$	—	$p = 0.11$	—	$p = 0.23$	—	$p = 0.77$	—	$p = 0.06$	—	$p = 0.80$	—			

To. Ellipse

Table 1. Circular statistics of microsaccade directions distributions for (columns) different categories of saccades (ALL: smaller than 1°; VS: between 0.1° and 0.5°; MS: between 0.5° and 1°; LS: between 1° and 2°, respectively, see text for details) and fixation periods (FP2a and FP2b) and (lines) stimulus sizes (SMALL and BIG). N is the number of microsaccades contained in each distribution (note that only subjects whose microsaccades were detected in both fixation periods were included for the statistical comparisons, for a particular category). The quantification of a bias in the direction of the ellipse major axis (to. ellipse) during all FP2a periods (except for LS) was done using the computation of the confidence intervals (bold font) of the actual distributions (or through the comparison between the median and the expected value of the bias—0—when circular uniformity could not be rejected, see Methods section). Note the absence of such a unique bias during all FP2b periods (except for VS-BIG stimulus): multi-directional biases (multi. bias) in directions oblique to that of the ellipse were observed here. Results of statistical comparisons between circular means (bold font) or between medians (italic font) of static and dynamic distributions are also provided: the type of noise almost never affected the shape of the microsaccade directions distribution.

Attention-related spatial changes

The static/dynamic amplitude ratios were close to one, and did not change across fixation periods ($p > 0.05$, see histograms in Figure 4A1, B1, C1, bottom panel). The search for a potential directional bias during task execution revealed a higher proportion of microsaccades in the direction of the ellipse major axis during task execution (FP2a—Figures 4A2, B2, left panel). Interestingly, this observation did not hold for LS saccades (Figure 4C2, left panel). For this last category, saccades were preferably generated along the oblique directions (vertical and horizontal directions on the screen). Such quadrimodal distributions were systematically observed after subjects' responses R1 (FP2b period, Figures 4A2, B2, C2, right panel) irrespective of the category under consideration.

These observations were confirmed by the results of the circular statistics comparisons presented in Table 1, where microsaccades never exhibited any significant bias towards the ellipse major axis direction during FP2b (except for the VS saccades for the BIG stimulus group). In contrast, such a significant bias was systematically reported for all but one (LS) category of saccades during the discrimination task execution (FP2a).

Taken together, these observations reveal that the noise-specific modulation of the microsaccade rate holds for saccades with larger amplitudes (although not significant for LS saccades and for VS saccades of the SMALL group, revealing an effect of the stimulus size). However, the directional bias observed during FP2a holds only for saccades with amplitudes smaller than 1° and is even stronger for saccades with amplitudes smaller than 0.5° (see FP2a distributions of VS-MS saccades in Figure 5A2, B2, left panel).

Microsaccadic activity and discrimination performance

The modulation of both microsaccade rates and orientations during FP2a may be driven by attention mechanisms devoted to gain information about the ellipse direction. If so, one would expect different patterns of changes in the case of incorrect compared to correct responses. We quantified this by separately analyzing microsaccades for correct and incorrect trials (Figure 5). Since subjects confirmed their first responses R1 in more than 96% of the cases, we extracted data based on R1 responses only. Besides, since comparable patterns of changes (see Figure 4A, B) were observed between VS and MS saccades, we compared here microsaccades with amplitude smaller than 1° (ALL) to LS saccades. Given the high discrimination performances (>84%), microsaccades detected for the incorrect trials were underrepresented compared to the

correct trials. This considerably reduced the size of the population for the statistical comparisons: Indeed, only subjects whose microsaccades were detected in all fixation periods were included for the statistical comparisons for a particular type of trial. For instance, VS microsaccades could not be detected during FP1, FP2a, or FP2b in 8 out of 33 subjects for the incorrect trials while this was the case in only one and four subjects for MS and LS saccades, respectively.

Attention-related temporal changes

The static/dynamic microsaccade rate ratios were systematically higher during FP2a versus FP1 (Figure 5-A1 through D1). However, this difference was significant only for ALL, $F(1, 33) = 16.9$, $p < 0.001$ and $F(1, 17) = 8.97$, $p < 0.01$ for correct and incorrect trials, but not for LS saccades ($p > 0.05$). They were significantly higher for ALL microsaccades during FP2a compared to FP2b for incorrect trials only, $F(1, 17) = 13.1$, $p < 0.01$. They were also significantly higher during FP2a for the SMALL stimulus for correct trials for both ALL and LS saccades, $F(1, 33) = 13.1$, $p < 0.001$ and $F(1, 29) = 12.0$, $p < 0.01$, respectively.

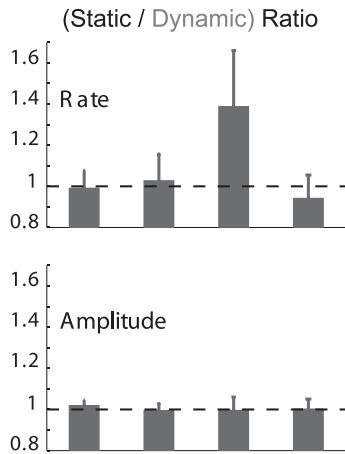
Attention-related spatial changes

As previously observed (Figure 3C, right panel and Figure 4C2), the distributions of microsaccade directions were biased along oblique directions during FP2b for both correct and incorrect trials (Figure 5A2 through D2, right panel). This was also the case during FP2a for LS saccades in both correct and incorrect trials (Figure 5C2, D2, left panel). Interestingly, the stimulus-driven bias observed for ALL microsaccades during FP2a was observed for correct trials only (Figure 5A2, left panel).

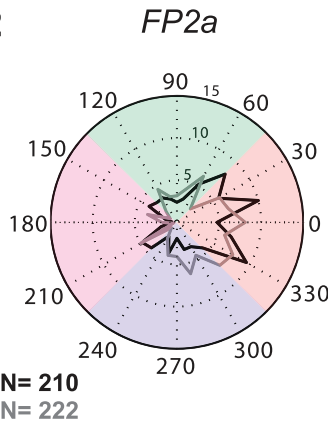
Such a bias was not observed for incorrect trials (Figure 5B2, left panel) where no systematic pattern of biases could be observed. This could be explained by a smaller number of microsaccades compared to correct trials: however, quadrimodal distributions were clearly visible for LS saccades (Figure 5D2, left and right panel) despite a number of saccades two times smaller than the one of ALL microsaccades (Figure 5B2, left panel). While this type of FP2a distribution of ALL microsaccades cannot easily be characterized, it is definitely different from the distributions observed for the correct trials (Figure 5A2, left panel). Besides, the circular statistics comparisons of the mean (or median) of static and dynamic distributions did not reveal any influence of noise ($p > 0.05$) for both incorrect and correct trials, except for two distributions of the SMALL group (ALL saccades/period 2a/correct trials and LS saccades/period 2b/incorrect trials distribu-

—— VS saccades (0.1 to 0.5 deg) ——

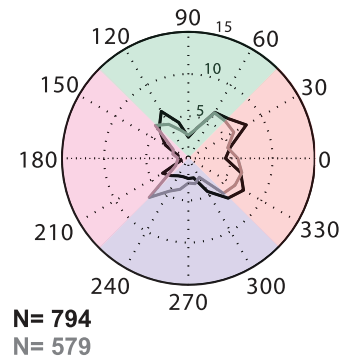
A1



A2

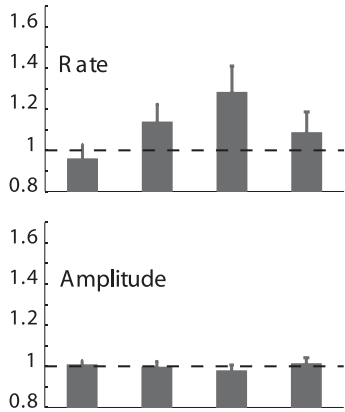


FP2b

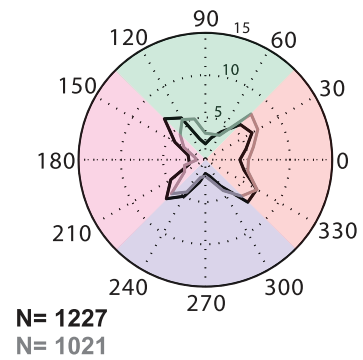
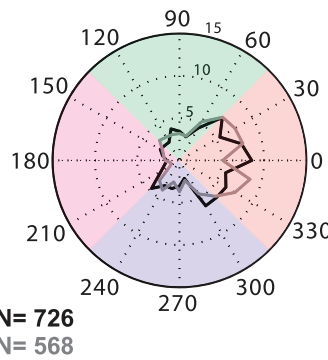


—— MS saccades (0.5 to 1 deg) ——

B1

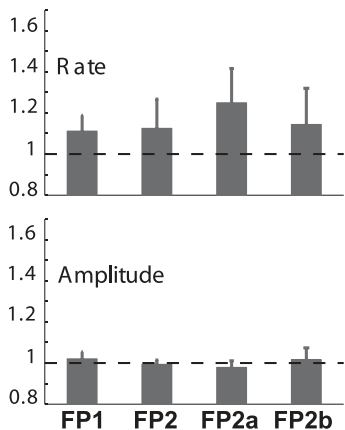


B2



—— LS saccades (1 to 2 deg) ——

C1



C2

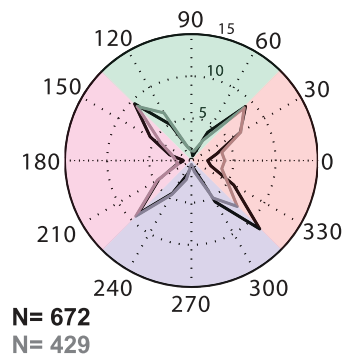
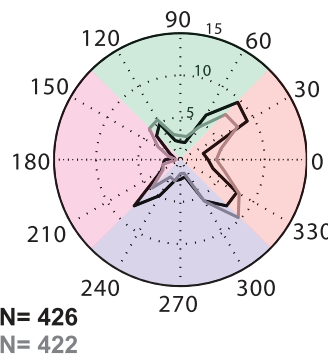
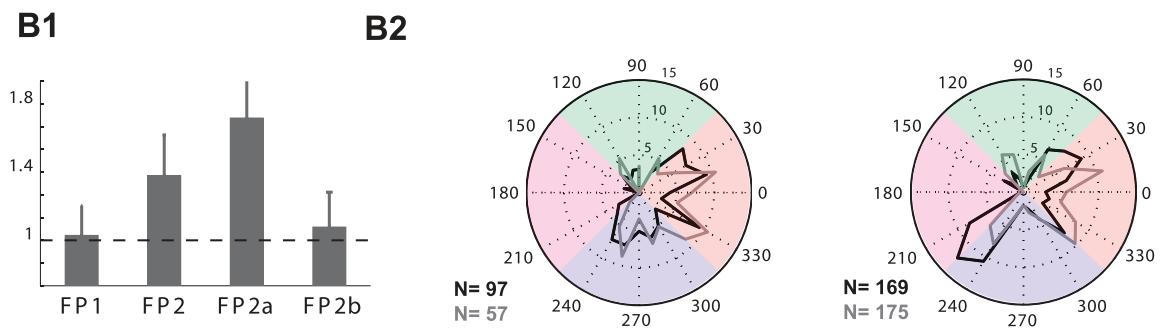
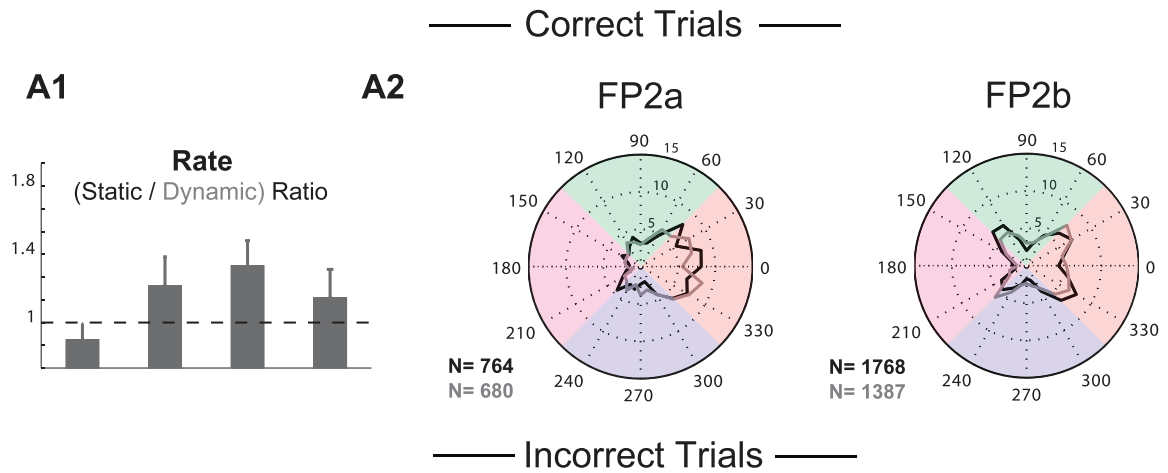


Figure 4. (A1, 2), (B1, 2), and (C1, 2): Same as Figures 4B, C but computed here for very small (VS), medium-size (MS), and larger (LS) saccades, respectively. Note that rates are significantly higher in the static condition during FP2a while amplitudes were not affected by noise, irrespective of the saccade amplitude. Note also the absence of any directional bias of saccades towards the stimulus direction during FP2a for LS in contrast with VS/MS saccades. See also Table 1.

Microsaccades (<1 deg)



LS saccades (1 to 2 deg)

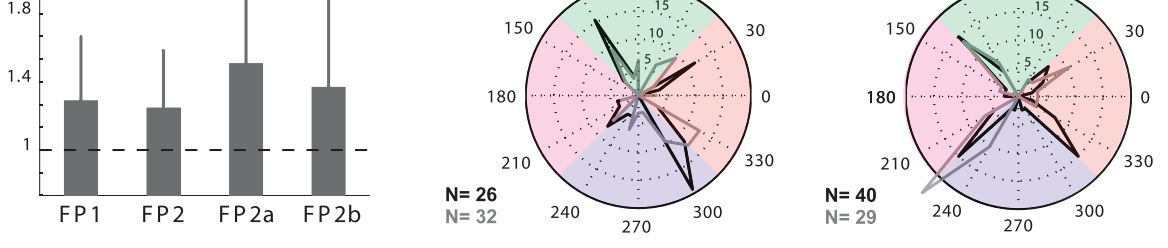
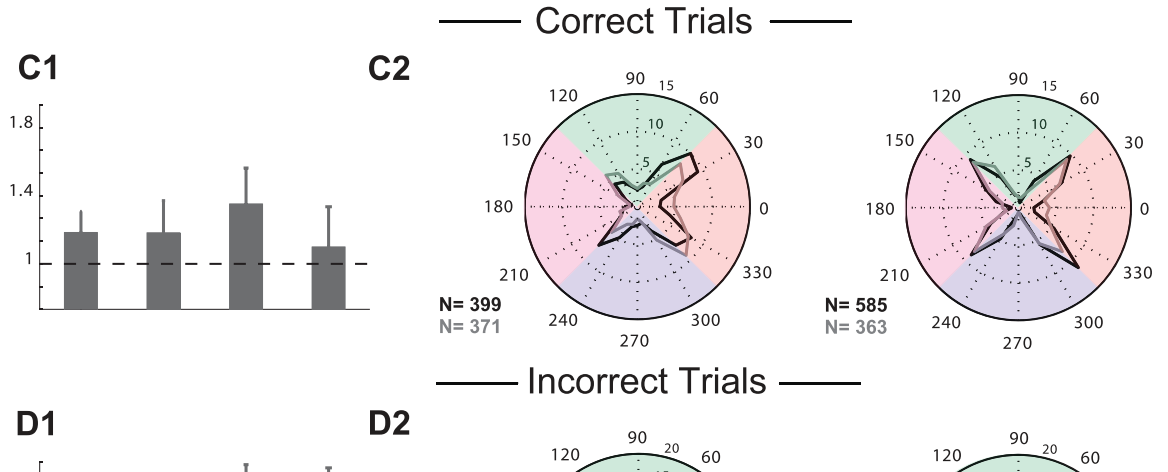


Figure 5. A1-B1 (C1, D1): Static/dynamic microsaccade rates ratios for correct and incorrect trials for ALL microsaccades (or LS saccades). A2-B2 (C2, D2): Microsaccade directions distributions for correct and incorrect trials for FP2a (left panel) and FP2b (right panel) periods.

tions, respectively) where the multisample test for equal median directions revealed a statistically significant difference between static and dynamic conditions, $P(1167) = 6.9$, $p = 0.008$ and $P(60) = 5.6$, $p = 0.018$, respectively.

Taken together, these observations further support the hypothesis that the microsaccadic modulation occurring during FP2a is devoted to gain information about the stimulus orientation. How microsaccades can contribute to improve discrimination performance is tested in the computational approach presented in the next section.

Modeling of the visual influence of background noise on microsaccades

We previously described a modulation of the microsaccadic activity driven by attentional demands and background noise. Here, we propose a computational approach based on a simple model of retinal photoreceptors (Zozor, Amblard, & Duchene, 2009). Our approach contrasts with more traditional models of microsaccades generation: while most of them focus on the activity of neural structures involved in microsaccades generation (Engbert, 2012; Engbert et al., 2011; Hafed, 2011; Hafed et al., 2009), we focus here on the output level, i.e., how the presence or absence of microsaccades affect spatial information acquisition at the retinal layer. It shall then be considered as a post-hoc explanation of the benefits of microsaccades in terms of visual information acquisition (but it definitely cannot account for the neural mechanisms underlying microsaccades generation).

Any dynamic change occurring in a tiny visual region may help in better discriminating stimuli: Microsaccades may represent one way to achieve this. Such potential noise-enhanced properties of microsaccades were recently modeled using a basic model of retinal photoreceptors (Zozor, Amblard, & Duchene, 2009). The terminology *noise-enhanced* denotes (in the signal processing area) the ability of systems to enhance their performances (information processing/acquisition/transmission/detection/discrimination/etc.) in the presence of noise. Since microsaccades generate rapid fluctuations in the retinal image, Zozor et al. (2009) suggested that these visual transients might be helpful in terms of spatial information processing. Here, we attempted to qualitatively reproduce the noise-specific effect on the microsaccadic activity. To this end, we implemented a modified version of this model (see Appendix for details) by simulating microsaccades on a time interval longer than that used in their study. This was done to account for the continuous sustained attention required for the execution of the discrimination task. Figure 6 depicts the discrimination perfor-

mance of an ideal observer (see Appendix) as a function of the microsaccade rate. We observed that the discrimination performances were systematically better in the dynamic than in the static situation in absence of microsaccades (for the zero value of the horizontal axis), regardless of the type of microsaccades directions distributions, as experimentally observed. This can be explained as follows: Since microsaccades produce changes in the noise structure of the acquired (otherwise static) image, they produce a noise-averaging process which results in a better discrimination performance in the dynamic condition. In other words, the presence of microsaccades (in the static condition) intermittently reproduces the effects of the dynamic background. Moreover, discrimination performances remained better in the dynamic condition over the whole range of simulated microsaccadic rates, with a peak around one, suggesting the existence of an optimal sampling rate associated with this noise averaging process.

Discussion

Several studies demonstrating that microsaccades may subserve functional roles during visual fixation have been published in the past 10 years. Here, we observed that the microsaccade rate was significantly modulated by the background noise only during the execution of a discrimination task. A directional bias of the microsaccades, dictated by the stimulus orientation, was temporally coupled with this period of increased activity. Both microsaccade rates and orientations were comparable across background types after the response time although subjects maintained fixation until the end of the trial. These observations may be related to several processes that are discussed below.

Background noise, discrimination task, and microsaccades

The microsaccade rate is significantly modulated by the perceptive visibility of a target (Cui, Wilke, Logothetis, Leopold, & Liang, 2009). In our study, the visibility of the ellipse might have been affected by background noise. However, subjects correctly perceived the ellipse orientation in more than 85% of the trials and their performances did not significantly differ across the tested conditions. Besides, we observed a significant modulation of the microsaccade rate (across conditions, see Figures 3B and 4A1, B1) during FP2a compared to FP2b although the visual background was identical during these two periods (the only difference being that subjects delivered their judgments at the end

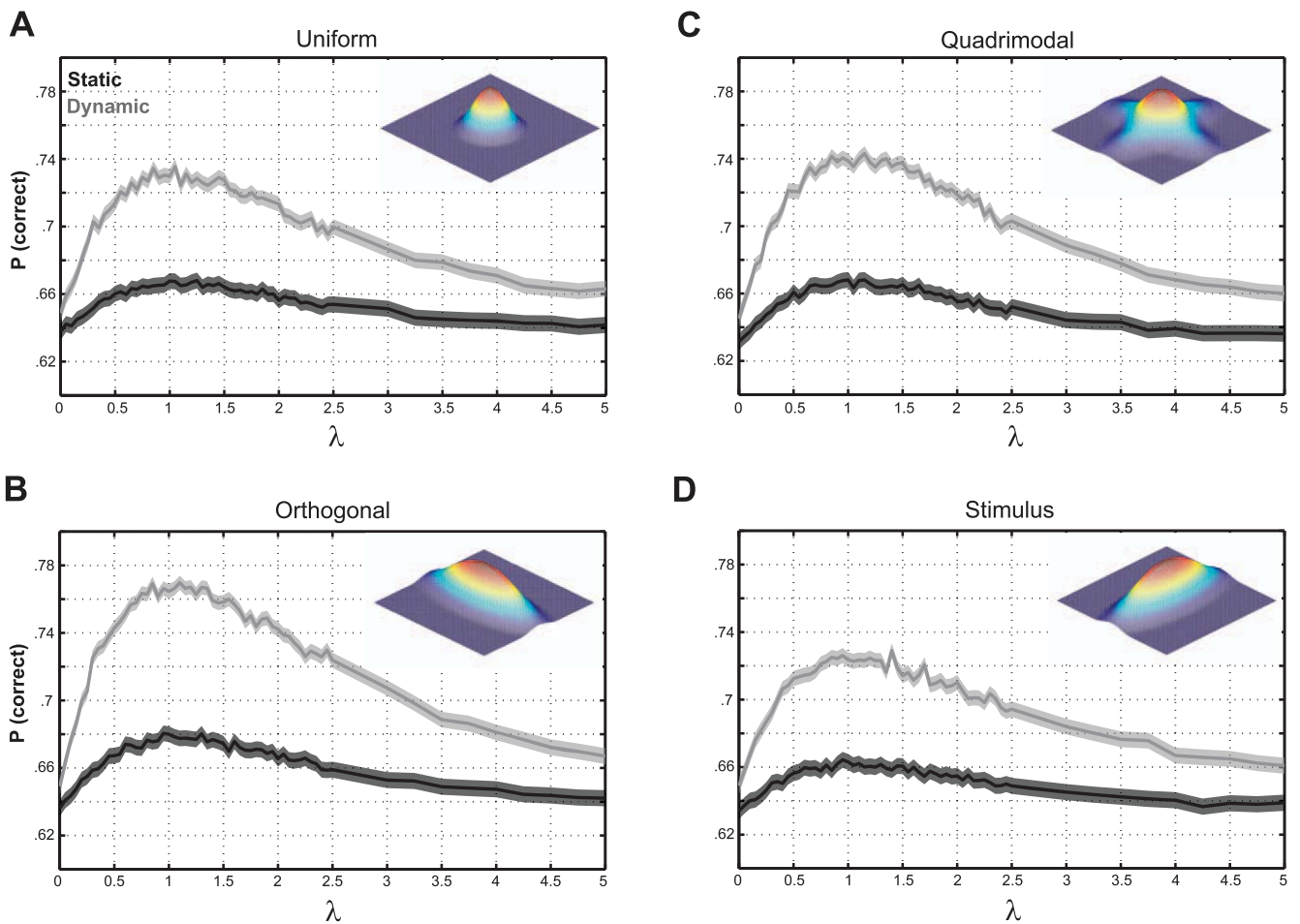


Figure 6. Estimated probability of taking the correct decision $P(\text{correct})$ versus the simulated microsaccade rate in the static (black line) and dynamic (gray line) conditions, for four types of microsaccade direction distributions (Note that only the quadrimodal and stimulus direction biased distributions were observed experimentally). Shadow regions around the mean curves represent the 95% confidence intervals, see text for details. More microsaccades are needed in the static condition to reach a discrimination performance similar to that of the dynamic condition. The probability distributions simulated to induce directional biases are inserted in the top-right panel of each plot (see Appendix for details).

of FP2a). Sinn and Engbert (2011) reported a stronger decrease of the microsaccade rate after stimulus presentation when testing structured versus uniform backgrounds. Here, we tested structured backgrounds and observed significant variations of the microsaccade rate depending on whether static or dynamic noise was present in the background. Besides, the background texture is not the only factor affecting the microsaccade activity. Indeed, the microsaccadic activity was significantly enhanced during FP2a only while the same visual stimulus was present across both FP2a and FP2b periods: This discards a purely visually driven effect. Microsaccade occurrences were thus greatly affected by attentional processes devoted to gain spatial information during task execution (FP2a). Such long-lasting task-related microsaccades modulation was also considered to be maintained by attentional demands (Pastukhov, Vonau, Stonkute, & Braun, 2012): Note

that despite a different paradigm, the experiments performed in this last study also required continuous sustained attention.

We tested whether the microsaccades-induced retinal motion facilitated the discrimination of the stimulus orientation through a simple model of photoretinal receptors being active throughout the discrimination task: Our simulations revealed that fewer microsaccades were necessary to reach a same level of performance in presence of dynamic noise. Furthermore, our model did not predict any changes induced by microsaccade direction distributions between static and dynamic background. Both of these predictions were observed experimentally. By contrast, the microsaccadic activity changes occurring at the transition between FP2a and FP2b could not be predicted by our model which did not include any attentional module.

The link between microsaccades and spatial information processing is also supported by the observed microsaccade orientations distributions. During FP2a, microsaccades were preferentially oriented in the direction of the stimulus orientation (especially for correct trials, see Figure 5A2 vs. 5B2) while they mostly followed a multimodal distribution (with biases along horizontal and vertical directions) during FP2b. This suggests that the modulation at work during FP2a was devoted to facilitate the judgment of the stimulus orientation.

Neuronal correlates and task dependency

Hafed et al. (2009) suggested that microsaccades are generated as a result of changes occurring in the bilateral retinotopic map of the superior colliculus (SC) during fixation: The allocation of attention to the periphery represents one of these sources causing asymmetry in the foveal activity of the SC, which eventually leads to microsaccade generation. However, this cannot explain the pattern of directional changes observed during the fixation on the stimulus. In fact, our paradigm forced subjects to scan a tiny visual region wherein stimuli were embedded. The attention level was probably higher while subjects were building their perceptual judgments (FP2a) compared to the subsequent period (FP2b) where they were waiting for the confirmation question (and did not spend too much effort in trying to judge the stimulus orientation—they indeed confirmed their first judgment in more than 96% of the cases). Thus, the particular demands of a task performed in such tiny region also determine the direction of microsaccades, probably through a modulation of attention. This may represent a distinct source of imbalances in the SC foveal activity, in addition to the allocation of attention to the periphery described above. At least, this confirms the existence of a visual strategy devoted to acquire spatial information in a tiny visual region through exploratory microsaccades (Ko, Poletti, & Rucci, 2010).

This exploratory function provides further evidence that microsaccades and saccades share common functional properties. In the last part of our study, we compared the properties of saccades based on their amplitudes. Interestingly, we observed that more saccades were generated in the presence of static backgrounds for all saccades with amplitude up to 2° (the difference was not significant for LS saccades). At the same time, the directional bias of microsaccades during FP2a was observed only for saccades with amplitudes smaller than 1° while those with larger amplitudes exhibited a preference for horizontal and/or vertical directions (see Engbert, 2006). Thus, saccades with amplitude less than 1° seem to have a specific

functional role related to our particular perceptual task. However, a directional bias of larger saccades may be observed depending on the size of the visual region. Further studies are required to specifically address the task-dependent microsaccadic changes.

Conclusion

We described here a background-specific modulation of the microsaccadic activity driven by attentional demands. A higher microsaccade rate was observed during fixation in presence of static backgrounds (compared to dynamic ones) only during the execution of a discrimination task. This resulted in comparable discrimination performances across visual conditions. The facilitating exploratory role of microsaccades could partly be achieved at the retinal layer, as illustrated by our computational predictions. However, the microsaccadic activity also exhibited a modulation driven by spatial attentional changes as evidenced by a stimulus-driven directional bias of microsaccades, also during the execution of a discrimination task only. Taken together, our experimental and theoretical findings further support the idea that microsaccades are under attentional control and represent an efficient sampling strategy allowing spatial information acquisition.

Keywords: ocular fixation, microsaccades, background noise, visual attention

Acknowledgments

This study was supported by the Agence Nationale pour la Recherche Grants VaRaD, ANR-JC09 494068 (AC) and ANR Gaze & EEG ANR-NT09_511856 (HH, AC, AC, SZ).

Commercial relationships: none.

Corresponding author: Halim Hicheur.

Email: halim.hicheur@unifr.ch.

Address: Department of Medicine, University of Fribourg, Fribourg, Switzerland.

References

- Berens, P. (2009). CircStat: A MATLAB toolbox for circular statistics. *Journal of Statistical Software*, 31(10), 1–21.
- Brodatz, P. (1966). *Textures: A photographic album for*

artists and designers. New York, NY: Dover Publications.

- Collewijn, H., & Kowler, E. (2008). The significance of microsaccades for vision and oculomotor control. *Journal of Vision*, 8(14):20, 1–21, <http://www.journalofvision.org/content/8/14/20>, doi:10.1167/8.14.20. [PubMed] [Article]
- Cui, J., Wilke, M., Logothetis, N. K., Leopold, D. A., & Liang, H. (2009). Visibility states modulate microsaccade rate and direction. *Vision Research*, 49(2), 228–236. doi:10.1016/j.visres.2008.10.015.
- Engbert, R. (2006). Microsaccades: A microcosm for research on oculomotor control, attention, and visual perception. *Progress in Brain Research*, 154, 177–192. doi:10.1016/S0079-6123(06)54009-9.
- Engbert, R. (2012). Computational modeling of collicular integration of perceptual responses and attention in microsaccades. *Journal of Neuroscience*, 32(23), 8035–8039. doi:10.1523/JNEUROSCI.0808-12.2012.
- Engbert, R., & Kliegl, R. (2003). Microsaccades uncover the orientation of covert attention. *Vision Research*, 43(9), 1035–1045.
- Engbert, R., & Mergenthaler, K. (2006). Microsaccades are triggered by low retinal image slip. *Proceedings of the National Academy of Sciences, USA*, 103(18), 7192–7197. doi:10.1073/pnas.0509557103.
- Engbert, R., Mergenthaler, K., Sinn, P., & Pikovsky, A. (2011). An integrated model of fixational eye movements and microsaccades. *Proceedings of the National Academy of Sciences, USA*, 108(39), E765–E770. doi:10.1073/pnas.1102730108.
- Feller, W. (1968). *An introduction to probability theory and its applications* (Vol. 1). New York: John Wiley & Sons.
- Hafed, Z. M. (2011). Mechanisms for generating and compensating for the smallest possible saccades. *European Journal of Neuroscience*, 33(11), 2101–2113. doi:10.1111/j.1460-9568.2011.07694.x.
- Hafed, Z. M., & Clark, J. J. (2002). Microsaccades as an overt measure of covert attention shifts. *Vision Research*, 42(22), 2533–2545.
- Hafed, Z. M., Goffart, L., & Krauzlis, R. J. (2009). A neural mechanism for microsaccade generation in the primate superior colliculus. *Science*, 323(5916), 940–943. doi:10.1126/science.1166112.
- Hafed, Z. M., Lovejoy, L. P., & Krauzlis, R. J. (2011). Modulation of microsaccades in monkey during a covert visual attention task. *Journal of Neuroscience*, 31(43), 15219–15230. doi:10.1523/JNEUROSCI.3106-11.2011.
- Hafed, Z. M., Lovejoy, L. P., & Krauzlis, R. J. (2013). Superior colliculus inactivation alters the relationship between covert visual attention and microsaccades. *European Journal of Neuroscience*, 37(7), 1169–1181, doi:10.1111/ejn.12127.
- Hafed, Z. M., & Ignashchenkova, A. (2013). On the dissociation between microsaccade rate and direction after peripheral cues: Microsaccadic inhibition revisited. *Journal of Neuroscience*, 33(41), 16220–16235. doi:10.1523/JNEUROSCI.2240-13.2013.
- Jammalamadaka Rao, S., & SenGupta, A. (2001). *Topics in circular statistics*. Singapore: World Scientific Publishing.
- Johnson, N. L., Kotz, S., & Kemp, A. W. (1992). *Univariate discrete distributions*. New York: John Wiley and Sons.
- Kay, S. M. (1998). *Fundamentals for statistical signal processing: Detection theory* (Vol. 2). Upper Saddle River, NJ: Prentice-Hall.
- Ko, H. K., Poletti, M., & Rucci, M. (2010). Microsaccades precisely relocate gaze in a high visual acuity task. *Nature Neuroscience*, 13(12), 1549–1553. doi:10.1038/nn.2663.
- Kotz, S., Balakrishnan, N., & Johnson, N. L. (2000). *Continuous multivariate distributions, vol. 1: Models and applications*. New York: John Wiley and Sons.
- Kuang, X., Poletti, M., Victor, J. D., & Rucci, M. (2012). Temporal encoding of spatial information during active visual fixation. *Current Biology*, 22(6), 510–514. doi:10.1016/j.cub.2012.01.050.
- Martinez-Conde, S., Macknik, S. L., Troncoso, X. G., & Dyar, T. A. (2006). Microsaccades counteract visual fading during fixation. *Neuron*, 49(2), 297–305. doi:10.1016/j.neuron.2005.11.033.
- McCamy, M. B., Otero-Millan, J., Macknik, S. L., Yang, Y., Troncoso, X. G., Baer, S. M., ... Martinez-Conde, S. (2012). Microsaccadic efficacy and contribution to foveal and peripheral vision. *Journal of Neuroscience*, 32(27), 9194–9204. doi:10.1523/JNEUROSCI.0515-12.2012.
- Mukhopadhyay, N. (2000). *Probability and statistical inference*. New York, NY: Marcel Dekker.
- Otero-Millan, J., Macknik, S. L., Serra, A., Leigh, R. J., & Martinez-Conde, S. (2011). Triggering mechanisms in microsaccade and saccade generation: A novel proposal. *Annals of the New York Academy of Sciences*, 1233, 107–116. doi:10.1111/j.1749-6632.2011.06177.x.
- Pastukhov, A., Vonau, V., Stonkute, S., & Braun, J. (2013). Spatial and temporal attention revealed by microsaccades. *Vision Research*, 85, 45–57, doi:10.1016/j.visres.2012.11.004.
- Poletti, M., & Rucci, M. (2010). Eye movements under

various conditions of image fading. *Journal of Vision*, 10(3):6, 1–18, <http://www.journalofvision.org/content/10/3/6>, doi:10.1167/10.3.6. [PubMed] [Article]

- Poletti, M., Listorti, C., & Rucci, M. (2013). Microscopic eye movements compensate for nonhomogeneous vision within the fovea. *Current Biology*, 23(17), 1691–1695, doi:10.1016/j.cub.2013.07.007.
- Rolfs, M. (2009). Microsaccades: Small steps on a long way. *Vision Research*, 49(20), 2415–2441. doi:10.1016/j.visres.2009.08.010.
- Rucci, M., & Casile, A. (2005). Fixational instability and natural image statistics: Implications for early visual representations. *Network-Computation in Neural Systems*, 16(2-3), 121–138. doi:10.1080/09548980500300507.
- Rucci, M., Iovin, R., Poletti, M., & Santini, F. (2007). Miniature eye movements enhance fine spatial detail. *Nature*, 447(7146), 851–854. doi:10.1038/nature05866.
- Sinn, P., & Engbert, R. (2011). Saccadic facilitation by modulation of microsaccades in natural backgrounds. *Attention, Perception, & Psychophysics*, 73(4), 1029–1033. doi:10.3758/s13414-011-0107-9.
- Smith, P. L., & Ratcliff, R. (2004). Psychology and neurobiology of simple decisions [Review]. *Trends in Neuroscience*, 27(3), 161–168. doi:10.1016/j.tins.2004.01.006.
- Steinman, R. M., Haddad, G. M., Skavenski, A. A., & Wyman, D. (1973). Miniature eye movement. *Science*, 181(4102), 810–819.
- Thaler, L., Schütz, A. C., Goodale, M. A., & Gegenfurtner, K. R. (2013). What is the best fixation target? The effect of target shape on stability of fixational eye movements. *Vision Research*, 76, 31–42.
- Van Horn, M. R., & Cullen, K. E. (2012). Coding of microsaccades in three-dimensional space by premotor saccadic neurons. *Journal of Neuroscience*, 32(6), 1974–1980. doi:10.1523/JNEUROSCI.5054-11.2012.
- Watson, A. B., & Pelli, D. G. (1983). Microsaccades during finely guided visuomotor tasks. *Vision Research*, 16(12), 1387–1390.
- Winterson, B. J., & Collewijn, H. (1976). QUEST: A Bayesian adaptive psychometric method. *Perception & Psychophysics*, 33(2), 113–120.
- Zozor, S., Amblard, P. O., & Duchene, C. (2009). Does eye tremor provide the hyperacuity phenomenon? *Journal of Statistical Mechanics-Theory and Experiment*, 1, 01015–01021, doi: Artn P01015 Doi 10.1088/1742-5468/2009/01/P01015

Zozor, S., & Vignat, C. (2010). Some results on the denoising Problem in the elliptically distributed context. *IEEE Transactions on Signal Processing*, 58(1).

Zuber, B. L., Stark, L., & Cook, G. (1965). Microsaccades and the velocity-amplitude relationship for saccadic eye movements. *Science*, 150(3702), 1459–1460.

Appendix

The aim of this model is to test for the presence of a potential noise-enhanced effect of microsaccades in presence of different noisy backgrounds. We originally modeled this effect at the level of individual photoreceptors for a single time frame (Zozor et al., 2009) based on the previous approach proposed by Rucci et al. (Rucci & Casile, 2005; Rucci et al., 2007). Here, the discrimination task is executed on a long time interval: from T noisy observations the decision H_{ccw} or H_{cw} could be made. The initial period of target fixation (FP1) was not considered here. Thus, we modified our previous model to account for the task duration, the microsaccade rate and the discrimination process, respectively.

Noise-free and noisy stimuli

The noise-free and noisy stimuli were the same as those used for the experiments (see Equation 1). Note that the absolute stimulus size was not important in our simulations: we set the relative size of the stimulus as half the size of the acquisition window and set $c = 0.06$.

Acquisition

We first assumed that (in absence of any microsaccade-related motion) the simulated sensor acquires a square subimage containing the stimulus. For each time frame t , this was implemented as proposed by Rucci et al. (Rucci & Casile, 2005; Rucci et al., 2007; and supplementary data in Kuang, Poletti, Victor, & Rucci, 2012; see also Zozor et al., 2009):

$$A(sx, t) = I\left(sx + \xi(t), t\right). \quad (2)$$

where s represents a subsampling coefficient that can account for the discrete nature of the grid of sensors and where the two-dimensional random signal $\xi(t)$ models the microsaccades (see next section). Note that at this step, we have not taken into account the processing performed by the cells (*spatiotemporal*

filtering, i.e., we focused here only on the acquisition level without dealing with any further processing).

Modeling of microsaccades properties

In contrast with the Brownian model proposed by Kuang et al. (2012), we considered here a compound nature of the noise and focused only on the microsaccades, ignoring the existence of other types of fixational eye movements. We first draw a set of random times of occurrences of microsaccades $\{T_k\}_{k>0}$. We then consider that the microsaccade is sustained during a time interval Δ_k (Otero-Millan et al., 2011). Finally, we randomly draw 2-D amplitudes Ξ_n for microsaccades occurring at times T_k . The microsaccadic activity takes then the form:

$$\xi(t) = \sum_{k \in N} \Xi_k 1_{[T_k; T_k + \Delta_k]}(t) \quad (3)$$

where 1_A denotes the indicator of set A , i.e., $1_A(t) = 1$ if $t \in A$ and $1_A(t) = 0$ otherwise.

The modeling of the rate, amplitudes, and directions of microsaccades was performed as follows. We computed microsaccade occurrence times using a punctual Poisson process (see also Engbert, 2012; Engbert et al., 2011): $T_k = \sum_{l=1}^k \tau_l^{(\lambda)}$ where $\tau_l^{(\lambda)}$ is a sequence of independent random variables following an exponential law of parameter λ (Feller, 1968; Johnson, Kotz, & Kemp, 1992). In other words, the epochs $T_{k+1} - T_k$ are independent and follow an exponential law of parameter λ . It appears then that the (random) number of events occurring in the time interval $[0; t]$ follows a Poisson law of parameter λt (Johnson, Kotz, & Kemp, 1992): λ is precisely the *microsaccade rate*, i.e., the average number of microsaccades per unit of time. Note that the assumption of a Poisson process for computing microsaccade occurrence is not exclusive (Hafed & Ignashchenkova, 2013) and does not affect our model's conclusions. We then fixed microsaccades durations Δ_k so that they are both independent and follow an uniform law over a certain interval (here $[2; 3]$ units of time). These durations are also assumed independent of the Poisson process $\{T_k\}$.

Finally, the *amplitude* Ξ_n of microsaccades is modeled as a mixture of two elliptically distributed Student- r laws, $f(\xi) = \alpha f_{R_0, v_0}(\xi) + (1 - \alpha) f_{R_1, v_1}(\xi)$, with $0 \leq \alpha \leq 1$ and where the Student-components (or Pearson type IIIa - see Kotz, Balakrishnan, & Johnson, 2000) write:

$$f_{R, v}(\xi) = \frac{v}{2(v+2)\pi |R|^{-\frac{1}{2}}} \left(1 - \frac{\xi^t R^{-1} \xi}{(v+2)} \right)_+^{v-1} \quad (4)$$

where v corresponds to the degrees of freedom, R is the covariance matrix of the bivariate random vector modeling the spatial microsaccadic component, $(\cdot)_+$ is

equal to $\max(\cdot, 0)$, and t stands for the transposition of a vector. For large values of v , a Student- r law behaves like a Gaussian (it tends to a Gaussian as $v \rightarrow \infty$), but it has a bounded support (note that a gamma distribution could also be used here). The term *elliptical* comes from the fact that the iso-probability contours (in Equation 4) are ellipses given by the equation $\xi^t R^{-1} \xi = \text{constant}$ (see Zozor & Vignat, 2010, for details). For R proportional to the identity, the distribution is isotropic while for the nonidentity, the main direction given by the eigenvectors of R^{-1} is privileged: This allowed us to model a *directional bias*. For $\alpha = 0$ or $\alpha = 1$, only one component remains. Otherwise, for appropriate choices of R_0 and R_1 (provided that R_0 and R_1 are not proportional) the bias is quadrimodal. Note that to obtain snapshots following such a mixture in the simulation, we computed each sample according to the first or second components with the probabilities α and $1 - \alpha$, respectively. In our simulation, we set $v = 4$ while the covariance matrices were chosen such that the large axes of each component were orthogonal in the mixture case.

We simulated four types of microsaccade direction distributions. The uniform (or isotropic—not observed experimentally) distribution was simulated by setting

$$R = \sigma^2 \begin{bmatrix} 1 & 0 \\ 0 & 1 \end{bmatrix},$$

with σ is half the size of the acquired subscene. The unimodal (or elliptic) distribution with a directional bias towards the ellipse major axis direction was simulated by setting

$$R = \sigma^2 \begin{bmatrix} \cos\theta & -\sin\theta \\ \sin\theta & \cos\theta \end{bmatrix} \begin{bmatrix} 1 & 0 \\ 0 & 15/7 \end{bmatrix} \begin{bmatrix} \cos\theta & \sin\theta \\ -\sin\theta & \cos\theta \end{bmatrix},$$

with θ being equal to the stimulus orientation. The unimodal (or elliptic) distribution with a directional bias orthogonal to the ellipse major axis (not observed experimentally) was simulated by setting R as previously but θ is here orthogonal to the stimulus orientation. The quadrimodal (or multi-axial) distributions were simulated by setting

$$R_0 = \sigma^2 \begin{bmatrix} 1 & 0 \\ 0 & 15/7 \end{bmatrix}$$

and

$$R_1 = \sigma^2 \begin{bmatrix} 15/7 & 0 \\ 0 & 1 \end{bmatrix}$$

and $\alpha = 0.5$.

Discrimination principle and performance

We performed the discrimination by projecting each observation on the noise-free stimulus, taking into account microsaccades. The T frames are projected on

the noise-free stimulus and summed to give the two statistics:

$$\Lambda_{cw,ccw} = \sum_{t,x} A(sx, t) I_{cw,ccw}(sx + \zeta(t)) \quad (5)$$

The decision H_{ccw} is made when $\Lambda_{ccw} > \Lambda_{cw}$, and reversely. The matched filter is the optimal linear discriminator between two deterministic signals (see Kay, 1998). Note that our goal was not to model the relationships between behavioral decisions and neuronal activity (as in Smith & Ratcliff, 2004, for instance). To assess the discrimination performance, we computed the probability of error (i.e., to take the wrong decision), that is formally expressed as:

$$P_e = \Pr \left[\text{decide } H_{ccw} \mid I_{nf} = I_{cw} \right] \cdot \Pr [I_{nf} = I_{cw}] \\ + \Pr \left[\text{decide } H_{cw} \mid I_{nf} = I_{ccw} \right] \cdot \Pr [I_{nf} = I_{ccw}] \quad (6)$$

We also computed the probability of correct responses as $P_g = 1 - P_e$.

Numerical simulations

The discriminations performances in the static and dynamic conditions were numerically assessed using a Monte Carlo method. We thus estimated P_g using $N_r = 10,000$ snapshots of the model for a period $T = 100$ frames (normalized fixation period during the discrimination task) for each value of λ we test. We independently draw the orientation of the noise-free stimulus, the background noise (static or dynamic), and microsaccades occurrences and amplitudes for each snapshot.

For each snapshot, we computed the matched filters $\Lambda_{cw,ccw}$ and compared them to make the decisions H_{ccw} or H_{cw} so that $\hat{P}_g = \frac{\text{number of good decisions}}{N_r}$. The 95% confidence interval was computed as

$$\left[\hat{P}_g - 1.96 \sqrt{\frac{\hat{P}_g(1 - \hat{P}_g)}{N_r}}; \hat{P}_g + 1.96 \sqrt{\frac{\hat{P}_g(1 - \hat{P}_g)}{N_r}} \right]$$

(Johnson et al., 1992; Mukhopadhyay, 2000).